

High efficiency, high energy, CEP-stabilized infrared optical parametric amplifier

This content has been downloaded from IOPscience. Please scroll down to see the full text.

2014 J. Opt. 16 102002

(<http://iopscience.iop.org/2040-8986/16/10/102002>)

View [the table of contents for this issue](#), or go to the [journal homepage](#) for more

Download details:

IP Address: 159.226.35.202

This content was downloaded on 19/12/2014 at 07:23

Please note that [terms and conditions apply](#).

Fast Track Communication

High efficiency, high energy, CEP-stabilized infrared optical parametric amplifier

Weijun Ling^{1,2}, Xiaotao Geng^{2,3}, Shuyan Guo⁴, Zhiyi Wei⁴, F Krausz^{5,6} and D Kim^{2,3}

¹ Department of Physics, Tianshui Normal University, Tianshui 741001, People's Republic of China

² Physics Department, & Center for Attosecond Science and Technology, POSTECH, 77 Cheongam-Ro, Nam-gu, Pohang, Gyeongbuk 790-784, Korea

³ Max Planck Center for Attosecond Science, Pohang, Gyeongbuk 790-784, Korea

⁴ Beijing National Laboratory for Condensed Matter Physics, Institute of Physics, Chinese Academy of Sciences, Beijing, People's Republic of China

⁵ Max-Planck-Institut für Quantenoptik, Hans-Kopfermann-Str.1, D-85748 Garching, Germany

⁶ Department for Physics, Ludwig-Maximilians-Universität, Am Coulombwall 1, D-85748 Garching, Germany

E-mail: kimd@postech.ac.kr

Received 7 June 2014, revised 10 August 2014

Accepted for publication 22 August 2014

Published 23 September 2014

Abstract

A high efficiency, tunable, carrier-envelope-phase (CEP) stabilized near-infrared optical parametric amplifier (OPA) is demonstrated with just a single BBO crystal. A white-light continuum produced by a CEP-stabilized laser is seeded into the two stages of the type II OPA system. We achieved a pump-to-signal conversion efficiency of 34% with a single nonlinear crystal. To our knowledge this is the highest conversion efficiency reported in broadband optical parametric amplification, using the two stages. This work demonstrates a compact way to for tunable femtosecond pulses with CEP stabilization.

Keywords: ultrafast nonlinear optics, parametric oscillators and amplifiers, ultrafast lasers, ultrafast technology

(Some figures may appear in colour only in the online journal)

1. Introduction

Powerful carrier-envelope-phase (CEP) stabilized pulses [1] that are tunable in the visible and/or near infrared spectral range are of special interest due to potential applications to nonlinear optics, ultrafast spectroscopy [1] and attosecond spectroscopy [2, 3]. Attosecond spectroscopy requires such pulses for the reproducible generation and precision measurement [4] of isolated attosecond pulses for pump-probe experiments. To this end, the higher pulses appear desirable, allowing the higher photon energy of the attosecond pulse according to the $I\lambda^2$ scaling of the cut-off energy of high-order harmonics (HOH), where I is the peak intensity and λ is the carrier wavelength [5]. Optical parametric amplification

(OPA) represents the most promising approach to achieving this goal [6–17].

At present, high energy pulses are generated mainly by non-collinear optical parametric amplifiers (NOPA) in β -barium borate (BBO) crystals [18–22] or collinear optical parametric amplifier (COPA) in BiB_3O_6 (BIBO) crystals [23, 24]. There are several ways to generate the broadband radiation needed to seed the OPA for powerful few-cycle pulse production. These include white light continuum (WLC) generation in a single filament in sapphire [18, 19], idler wave generation in a non-collinear OPA, difference-frequency generation (DFG) with the supercontinuum emerging from a hollow-core fiber [21, 22], a sapphire plate [23, 24], PPLN [25] or YAG [26]. Such a broadband seed pulse has then been amplified by two or three OPA stages in

previous works. For tunable femtosecond OPAs based on BBO, BIBO and LBO crystals, overall pump-to-signal conversion efficiencies of about 20% have been reported [24, 27–31]. LBO (as a nonlinear crystal) resulted in the highest pump to signal conversion efficiency of 34% in a 250 mJ, 5 Hz OPCPA system pumped by a laser with engineered spatial and temporal beam profiles [32]. However, LBO is not the ideal choice for few-cycle OPA due to its unfavorable gain-bandwidth limit. NOPA implemented with BBO crystals as the nonlinear medium is ideally suited for efficient broadband amplification. Using BBO crystals, a few mJ, kHz OPCPA systems were recently reported in a broadband optical parametric amplification by a careful optimization of the pump intensity in the crystal [33, 34].

CEP stabilization is indispensable for optical frequency synthesis [35], precision attosecond metrology, spectroscopy, and control [1, 4, 36–38]. Active and passive technologies have been developed for producing CEP-controlled pulses. The active scheme requires that CEP stabilization be realized by active electronic control loops based on pulse measurements of the pulse phase slips of the oscillator [4, 6–9]. DFG naturally produces pulses with constant CEP from any pulse with uncontrolled CEP, resulting in a passive CEP stabilization [10–17]. Both pump and seed from a non-CEP-stabilized laser are suitable for a passive CEP stabilized OPA. An OPA driven by a pump and seeded with a signal that are derived from the same (non-CEP-stabilized) radiation yields a (passively) CEP-stabilized idler wave that can be further amplified for powerful CEP-stable pulse generation [39]. Passive CEP stabilization do not require fast feedback loops but generally do rely on active stabilization against slow drifts of the CEP in the amplified output.

In this work, we report a tunable near-infrared OPA system, with an (pump to signal) conversion efficiency of 34%, CEP stabilization and easy tuning. A white-light continuum produced by a CEP stabilized laser is seeded into the two stages of the type II OPA system. We opted for type II phase matching owing to its favorable properties such as easy separation of signal and idler wave due to their different polarizations, high conversion efficiency due to opposite relative group velocity of signal and idler wave with respect to group velocity of the pump, and constant bandwidth, independent of the center wavelength of the signal [18]. Thanks to the (actively) CEP-stabilized seed, we can avoid any beam degradation that might originate from the idler angle dispersion in the OPA process or the difficulty of separating beams in the DFG process in the passive CEP schemes. A tunable output requires that the nonlinear crystals in different OPA stages be precisely temporal overlapped and rotated for the same angle and usually mounted on precision rotation mounts with a step motor drive. In order to avoid these difficulties and complications, we have implemented OPA with only one BBO crystal for a two-stage amplification, for an easy and user-friendly time-overlap adjustment of the two OPA stages.

A pulse energy of up to 138 μJ at 1350 nm has been obtained at a pump energy of 407 μJ . This corresponds to a pump-to-signal conversion efficiency of 34%. The CEP jitter

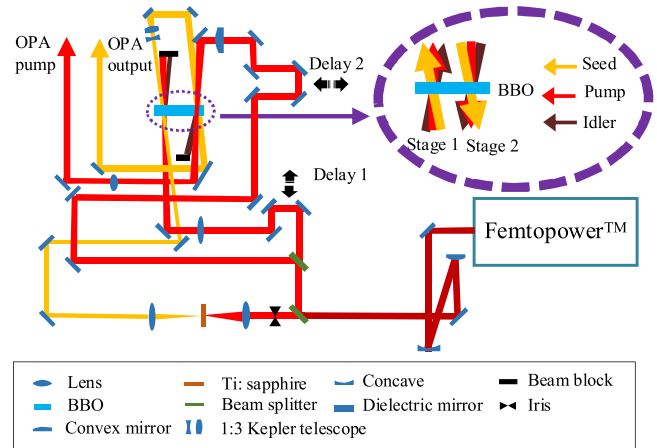


Figure 1. Schematic of the experimental setup for the generation of hybrid CEP stable pulses based on two-stages NOPA. Inset: schematic diagram of optical path in a single BBO crystal.

of amplified signals is measured to be 117 mrad by a spectral interferometry based on $f-2f$ principle. The scheme demonstrates a simple and efficient way to generate tunable femtosecond IR laser pulses with a stabilized CEP.

2. Experimental setup

Figure 1 shows the experimental layout of the two-stage NOPA setup. A commercial Ti: sapphire multi-pass chirped-pulse-amplification (CPA) laser system (with active CEP stabilization) is used as a pump source to provide 25 fs laser pulses with an energy of 510 μJ at a repetition rate of 3 kHz and a central wavelength of 800 nm (Femtopower™ from Femto lasers). The experimental setup consists of three parts: WLC generation and two NOPA amplification stages. The driving pulse is split into three parts by two beam splitters (BS). A fraction of the driving pulses (3 μJ) is taken and focused onto a 2 mm thick sapphire plate. An iris placed before the focus lens controls the energy in the sapphire plate and generates a single filament WLC with excellent radial intensity. About 1 μJ of energy is focused into the sapphire plate by a lens with $f = 100$ mm; subsequently, a WLC with excellent beam quality is produced. This is used as the seed for the stage 1. About 100 μJ of energy is split by a beam splitter (with a splitting ratio of 1:5) and focused with an $f = 500$ mm lens to pump the stage 1. A 3 mm-thick BBO crystal with an aperture of 17 mm \times 17 mm is used in the stage 1, which is cut with a phase matching angle at $\theta = 28^\circ$, $\phi = 30^\circ$ for type II ($e(\text{pump}) \rightarrow e(\text{signal}) + o(\text{idler})$) phase matching. We introduce a 1.7° non-collinear angle (internal) between the pump and the signal. To avoid damaging the parametric crystal or restraining superfluorescence, the beam diameter of the pump laser in the BBO crystal is controlled to be about 1.4 mm by a convex lens ($f = 500$ mm), corresponding to an intensity of 260 GW cm^{-2} .

3. Results and discussion

An amplified signal energy of $3 \mu\text{J}$ is obtained in stage 1. We expand and collimate the seed beam with a Kepler 1:3 telescope to match the beam size of the seed and the pump pulses on the crystal for stage 2. The idler wave is blocked by a beam dump when it is separated from seed and pump laser after propagation. Then the collimated signal output from stage 1 is injected into stage 2 for further amplification, in which the signal and pump light are incident on the same BBO in the opposite direction and parallel to each other as in stage 1. The optical path in the BBO is shown by the inset of figure 1. About $407 \mu\text{J}$ is sent to pump the stage 2 by the second beam splitter. To obtain the best spatial beam quality for the output pulse, the power density on the crystal is optimized by a down-collimator with a ratio of 3:1. We carefully optimize the spatial and temporal match by adjusting the crystal phase matching angle and the time delay for pump pulses in order to obtain a stable amplification in the saturation regime. We measure as much as $138 \mu\text{J}$ of amplified signal energy directly after the nonlinear crystal that corresponds to the pump-to-signal conversion efficiency of 34%.

In the stage 2, the tunable signal pulse is amplified and signal spectrum can be tuned from 1100 nm to 1700 nm by changing BBO phase matching angle, (see figure 2(a)). Figure 2(b) is the conversion efficiency curve corresponding to different signal wavelengths measured by changing phase matching angle. The conversion efficiency varies from 12% around 1100 nm and 1700 nm to 34% around 1350 nm.

The pulse duration of OPA output is determined by the pump pulse width. The pulse is characterized by spectral phase interferometer for the direct electric field reconstruction (SPIDER) method. Figure 2(c) shows the reconstructed pulse in the time domain, which has a full width at half maximum (FWHM) duration of 28 fs around 1350 nm and is comparable to a pump pulse duration of 25 fs FWHM. The result indicates that the amplified pulse duration does not change relative to the pump pulse duration in the IR wavelength range.

It is necessary to restrain the superfluorescent amplified signal (SAS) in order to obtain a good signal beam quality in stage 2. To do so, the pump intensity for the stage 2 is controlled at 250 GW cm^{-2} . Simultaneously, we found that the optimization of timing overlap between the signal and pump is important to improve beam quality. Figures 3(a) and (b) show the amplified signal beam quality at different times of timing overlap. The bad beam quality in figure 3(a) is due to imperfect timing overlap with a strong SAS. A precise pump and signal time overlap removes most of the SAS and obtains a perfect beam quality (see figure 3(b)).

In the current tuning range of the spectrum, the sign of the relative group velocity of the signal wave with respect to the pump is opposite to that of the relative group velocity of the idler wave with respect to the pump. The simulation study shows that the exponential growth of the signal is preserved for a long length of crystal [40]. This fact relaxes the restriction on the crystal length (the typical separation length of 2 mm for 790 nm pumping) due to group-velocity

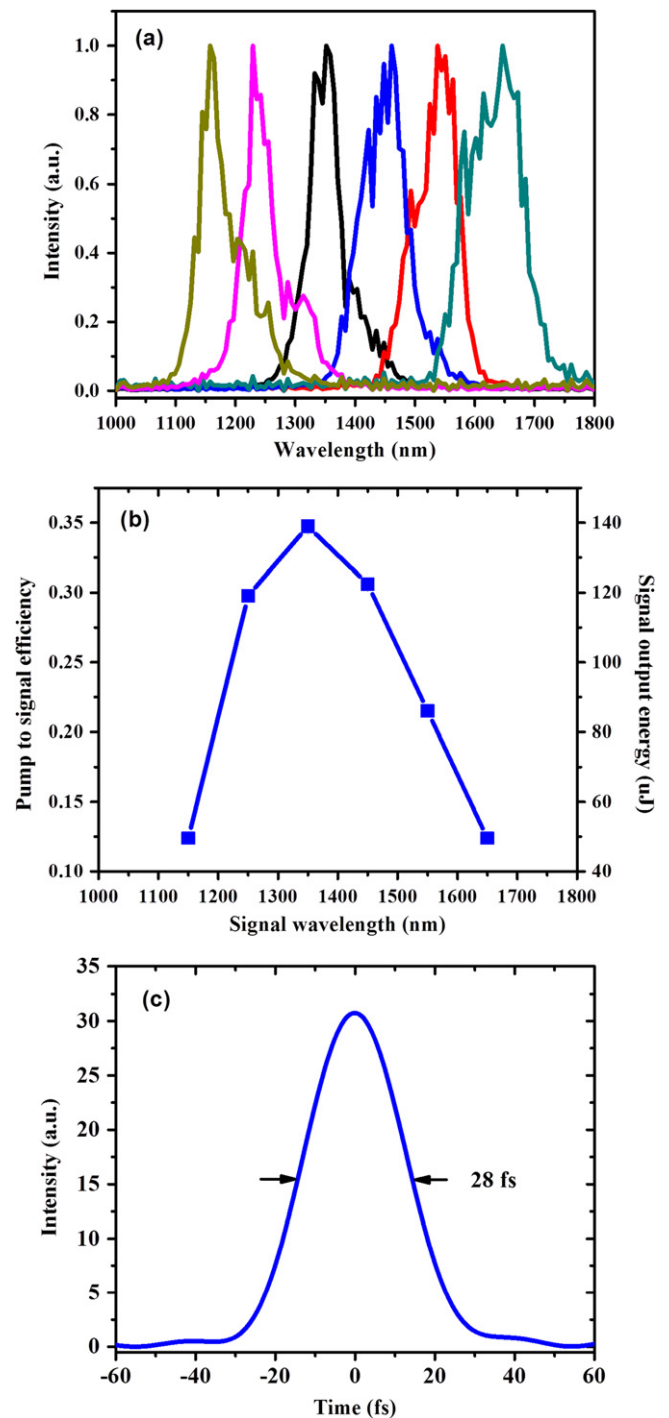


Figure 2. (a) (Normalized) spectrum change of the optical parametric amplifier by changing BBO phase matching angle. (b) The pump to signal conversion efficiency curve in the final OPA stage. The highest conversion efficiency is 34% for the signal pulses at 1350 nm. (c) Reconstructed pulse in the time domain around 1350 nm measured by SPIDER method.

mismatch. A longer crystal can result in a higher conversion efficiency. Hence a 3 mm thick BBO is selected, which has a minimal effect on pulse broadening of the seed laser and yet results in a high conversion efficiency. The same gain wavelength in a two-stages NOPA (because the angle between the pump and the signal light as well as between the

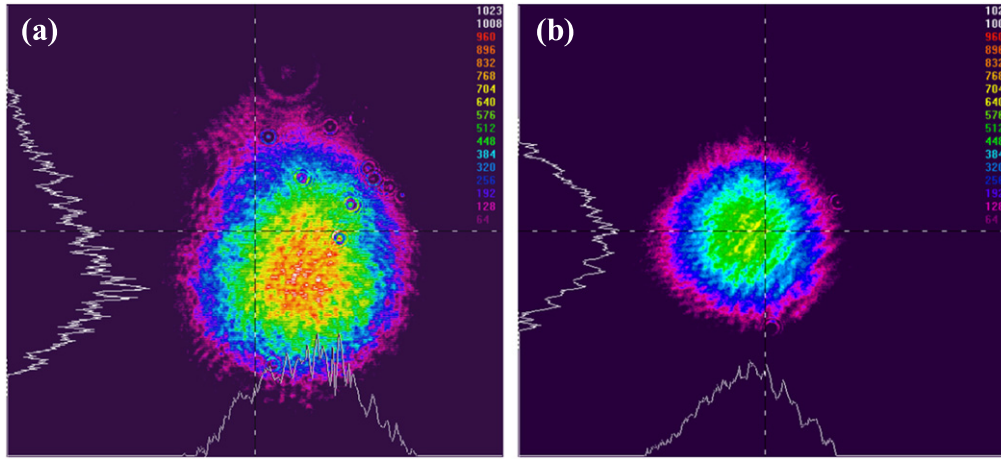


Figure 3. (a) Final amplified pulse profile with SAS; (b) final amplified pulse profile with perfect temporal overlap.

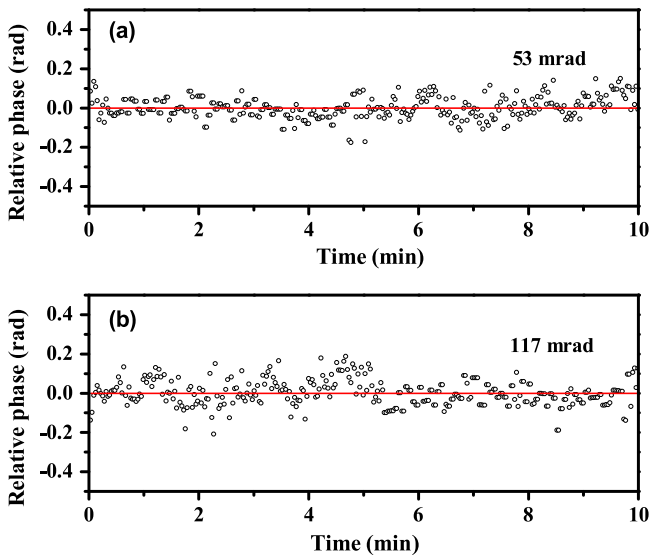


Figure 4. CEP jitter fluctuation over time (a) seed light CEP jitter is 53 mrad (rms); (b) the final amplified pulse CEP jitter is 117 mrad (rms).

crystal and the pump are maintained the same as shown in the inset of figure 1) also contributes to the high conversion efficiency. Excellent quality of pump and signal beams as well as their spatial and temporal matching are also important prerequisites for the high efficiency obtained.

To investigate the effect of NOPA on maintaining a stable CEP in the amplified output, we use an $f-2f$ interferometer and measure the CEP jitter of the seed as well as the amplified pulse after the stage 2. The $f-2f$ interferometric spectra are recorded with a time interval of 10 min (see figure 4). The linear Fourier-transform spectral interferometry algorithm analysis of the spectral interference fringes with 50 ms time shows that the CEP jitter is 53 mrad (rms) for seed pulse and 117 mrad (rms) for amplified signals. Hence, the CEP jitter is increased by approximately a factor of two in the OPA process. The result shows that the CEP hybrid control method (based on the active control of seed pulse CEP and the passive control of amplified pulse CEP) is feasible and

effective for CEP controlled infrared NOPA. For practical applications, we need the CEP to be kept stable for hours. Since the seed pulse CEP is actively controlled in this hybrid control scheme, we can easily set up a slow loop to control output pulse CEP for a longer period of time. This is the advantage of the current hybrid scheme. If seed pulse CEP comes from passive method, output pulse CEP cannot be controlled by active method.

4. Conclusion

We developed a high efficiency, high energy, tunable phase-stabilized near-infrared femtosecond OPA at 3 kHz, which consists of a WLC stage and two non-collinear OPA stages with only one amplification medium (BBO). A hybrid control method stabilized the CEP of the tunable output pulses. The tunable output pulses were still CEP-stabilized by an actively CEP-stabilized seed and pump pulse. A single BBO crystal demonstrated a high efficiency two-stage NOPA. The highest conversion efficiency of 34% was achieved at 1350 nm in type II phase matching condition. The total tunable spectral range for the signal pulses was from 1100 nm to 1700 nm. The measured CEP jitter of the output pulses from the OPA was 117 mrad (rms) for an input jitter of 53 mrad. The maintenance of the stability of about 100 mrad over a longer period of time may require a slow feedback loop for suppressing possible slow drifts of CEP likely to occur over a period of tens of minutes or beyond. The single crystal configuration provides a simple and efficient way to produce tunable femtosecond pulses, leading to a compact system.

The laser light around 1350 nm has a 3 times larger ponderomotive potential than the 800 nm light. Hence the fs laser pulse around 1350 nm is capable to generate HOH in the water window region. The recent simulation study on two color scheme for the generation of isolated attosecond pulse [41] shows that the proper mixing of a weak fs light around 1300 nm with a strong 800 nm fs light can lead to the generation of isolated attosecond pulse using a rather long fs pulse.

The fs OPA laser around 1350 nm not only is used immediately to these two examples but also will find applications in various areas.

Acknowledgment

This research has been supported by Global Research Laboratory Program (Grant No 2011-00131), by Leading Foreign Research Institute Recruitment Program (Grant No 2010-00471) and by Max Planck POSTECH/KOREA Research Initiative Program (Grant No 2011-0031558) through the National Research Foundation of Korea (NRF) funded by Ministry of Science, ICT & Future Planning The work is also supported by the National Natural Science Foundation of China (NO. 61465012, NO. 60608003, NO. 60878020, and NO. 10874237), and the Instrument Developing Project of the Chinese Academy of Sciences (Grant No. 2010004). Cooperation between the three participating groups has also been greatly stimulated and facilitated by the Max-Planck-Center for Attosecond Science funded by the Max Planck Society.

References

- [1] Baltuška A *et al* 2003 Attosecond control of electronic processes by intense light fields *Nature* **421** 611–5
- [2] Krausz F and Ivanov M 2009 Attosecond physics *Rev. Mod. Phys.* **81** 163–234
- [3] Hentschel M, Kienberger R, Spielmann C, Reider G A, Milosevic N, Brabec T, Corkum P, Heinzmann U, Drescher M and Krausz F 2001 Attosecond metrology *Nature* **414** 509–13
- [4] Kienberger R *et al* 2004 Atomic transient recorder *Nature* **427** 817–28
- [5] Hernández-García C, Pérez-Hernández J A, Popmintchev T, Murnane M M, Kapteyn H C, Jaron-Becker A, Becker A and Plaja L 2013 Zeptosecond high harmonic keV x-ray waveforms driven by midinfrared laser pulses *Phys. Rev. Lett.* **111** 033002
- [6] Cundiff S T 2002 Phase stabilization of ultrashort optical pulses *J. Phys. D: Appl. Phys.* **35** 43–59
- [7] Chang Z H 2006 Carrier-envelope phase shift caused by grating-based stretchers and compressors *Appl. Opt.* **45** 8350–3
- [8] Gagnon E, Thomann I, Paul A, Lytle A, Backus S, Murnane M, Kapteyn H and Sandhu A 2006 Long-term carrier-envelope phase stability from a grating-based, chirped pulse amplifier *Opt. Lett.* **31** 1866–8
- [9] Li C Q, Moon E and Chang Z H 2006 Carrier-envelope phase shift caused by variation of grating separation *Opt. Lett.* **31** 3113–5
- [10] Fuji T, Apolonski A and Krausz F 2009 Self-stabilization of carrier-envelope offset phase by use of difference-frequency generation *Opt. Lett.* **29** 632–4
- [11] Manzoni C, Vozzi C, Benedetti E, Sansone G, Stagira S, Svelto O, De Silvestri S, Nisoli M and Cerullo G 2006 Generation of high-energy self-phase-stabilized pulses by difference-frequency generation followed by optical parametric amplification *Opt. Lett.* **31** 963–5
- [12] Manzoni C, Cerullo G and De Silvestri S 2004 Ultrabroadband self-phase-stabilized pulses by difference-frequency generation *Opt. Lett.* **29** 2668–70
- [13] Cirmi G, Manzoni C, Brida D, De Silvestri S and Cerullo G 2008 Carrier-envelope phase stable, few-optical-cycle pulses tunable from visible to near IR *J. Opt. Soc. Am. B* **25** 62–9
- [14] Baltuška A, Fuji T and Kobayashi T 2002 Controlling the carrier-envelope phase of ultrashort light pulses with optical parametric amplifiers *Phys. Rev. Lett.* **88** 133901
- [15] Homann C, Bradler M, Förster M, Hommelhoff P and Riedle E 2012 Carrier-envelope phase stable sub-two-cycle pulses tunable around 1.8 μm at 100 kHz *Opt. Lett.* **37** 1673–5
- [16] Darginavičius J, Garejev N and Dubietis A 2012 Generation of carrier-envelope phase-stable two optical-cycle pulses at 2 μm from a noncollinear beta-barium borate optical parametric amplifier *Opt. Lett.* **37** 4805–7
- [17] Bradler M, Homann C and Riedle E 2013 Broadband difference frequency mixing between visible and near-infrared pulses for few-cycle pulse generation with stable carrier-envelope phase *Appl. Phys. B* **113** 19–25
- [18] Wilson K R and Yakovlev V V 1997 Ultrafast rainbow: tunable ultrashort pulses from a solid-state kilohertz system *J. Opt. Soc. Am. B* **14** 444–8
- [19] Cerullo G and De Silvestri S 2003 Ultrafast optical parametric amplifiers *Rev. Sci. Instrum.* **74** 1–18
- [20] Zhang C, Wei P, Huang Y, Leng Y, Zheng Y, Zeng Z, Li R and Xu Z 2009 Tunable phase-stabilized infrared optical parametric amplifier for high-order harmonic generation *Opt. Lett.* **34** 2730–2
- [21] Vozzi C *et al* 2006 High-energy, few-optical-cycle pulses at 1.5 μm with passive carrier-envelope phase stabilization *Opt. Express* **14** 10109–16
- [22] Vozzi C, Calegari F, Benedetti E, Gasilov S, Sansone G, Cerullo G, Nisoli M, De Silvestri S and Stagira S 2007 Millijoule-level phase-stabilized few-optical-cycle infrared parametric source *Opt. Lett.* **32** 2957–9
- [23] Silva F, Bates P K, Esteban-Martin A, Ebrahim-Zadeh M and Biegert J 2012 High-average-power, carrier-envelope phase-stable, few-cycle pulses at 2.1 μm from a collinear BiB₃O₆ optical parametric amplifier *Opt. Lett.* **37** 933–5
- [24] Ghotbi M, Beutler M, Petrov V, Gaydardzhiev A and Noack F 2009 High-energy, sub-30 fs near-IR pulses from a broadband optical parametric amplifier based on collinear interaction in BiB₃O₆ *Opt. Lett.* **34** 689–91
- [25] Fuji T, Ishii N, Teisset C Y, Gu X, Metzger T, Baltuška A, Forget N, Kaplan D, Galvanauskas A and Krausz F 2006 Parametric amplification of few-cycle carrier-envelope phase-stable pulses at 2.1 μm *Opt. Lett.* **31** 1103–5
- [26] Bradler M, Baum P and Riedle E 2009 Femtosecond continuum generation in bulk laser host materials with sub- μJ pump pulses *Appl. Phys. B* **97** 561–74
- [27] Sun Z, Ghotbi M and Ebrahim-Zadeh M 2007 Widely tunable picosecond optical parametric generation and amplification in BiB₃O₆ *Opt. Express* **15** 4139–48
- [28] Chekhlov O V *et al* 2006 35 J broadband femtosecond optical parametric chirped pulse amplification system *Opt. Lett.* **31** 3665–7
- [29] Ghotbi M, Ebrahim-Zadeh M, Petrov V, Tzankov P and Noack F 2006 Efficient 1 kHz femtosecond optical parametric amplification in BiB₃O₆ pumped at 800 nm *Opt. Express* **14** 10621–6
- [30] Zhang J, Zhang Q L, Zhang D X, Feng B H and Zhang J Y 2010 Generation and optical parametric amplification of picosecond supercontinuum *Appl. Opt.* **49** 6645–50
- [31] Waxer L J, Bagnoud V, Begishev I A, Guardalben M J, Puth J and Zuegel J D 2003 High-conversion-efficiency optical parametric chirped-pulse amplification system using spatiotemporally shaped pump pulses *Opt. Lett.* **28** 1245–7

- [32] Bagnoud V, Begishev I A, Guardalben M J, Puth J and Zuegel J D 2005 5 Hz, >250 mJ optical parametric chirped-pulse amplifier at 1053 nm *Opt. Lett.* **30** 1843–5
- [33] Fattahi H, Skrobol C, Ueffing M, Deng Y, Schwarz A, Kida Y, Pervak V, Metzger T, Major Z and Krausz F 2012 High efficiency, multi-mJ, sub 10 fs, optical parametric amplifier at 3 kHz *Conf. on Lasers and Electro-Optics (CLEO): Science and Innovations* CThN.6
- [34] Ding C, Xiong W, Fan T, Hickstein D D, Popmintchev T, Zhang X, Walls M, Murnane M M and Kapteyn H C 2014 High flux coherent supercontinuum soft x-ray source driven by a single-stage, 10 mJ, Ti:sapphire amplifier-pumped OPA *Opt. Express* **22** 6194
- [35] Jones D J, Diddams S A, Ranka J K, Stentz A, Windeler R S, Hall J L and Cundiff S T 2000 Carrier-envelope phase control of femtosecond mode-locked lasers and direct optical frequency synthesis *Science* **288** 635–9
- [36] Sansone G *et al* 2006 Isolated single-cycle attosecond pulses *Science* **314** 443–6
- [37] Schultze M, Goulielmakis E, Uiberacker M, Hofstetter M, Kim J, Kim D, Krausz F and Kleineberg U 2007 Powerful 170-attosecond XUV pulses generated with few-cycle laser pulses and broadband multilayer optics *New J. Phys.* **9** 243
- [38] Zherebtsov S *et al* 2011 Controlled near-field enhanced electron acceleration from dielectric nanospheres with intense few-cycle laser fields *Nat. Phys.* **7** 656–62
- [39] Manzoni C, Polli D, Cirmi G, Brida D, De Silvestri S and Cerullo G 2007 Tunable few-optical-cycle pulses with passive carrier-envelope phase stabilization from an optical parametric amplifier *Appl. Phys. Lett.* **90** 171111
- [40] Danielius R, Piskarskas A, Stabinis A, Banfi G P, Di Trapani P and Righini R 1993 Traveling-wave parametric generation of widely tunable, highly coherent femtosecond light pulses *J. Opt. Soc. Am. B* **10** 2222–32
- [41] Kim B, Ahn J, Yu Y, Cheng Y, Xu Z and Kim D 2008 Optimization of multi-cycle two-color laser fields for the generation of an isolated attosecond pulse *Opt. Express* **16** 10331–40